MARY KAY O'CONNOR PROCESS SAFETY CENTER
TEXAS A&M ENGINEERING EXPERIMENT STATION

19th Annual International Symposium
October 25-27, 2016 • College Station, Texas

Accounting for Channeling and Shielding Effects for Vapor Cloud Explosions

James Wesevich*, P. Hassig, L. Nikodym, V. Nasri, and J. Mould
Thornton Tomasetti, Weidlinger Applied Science
115 Wild Basin Road, Suite 309
Austin, Texas 78746
*Presenter E-mail: JWesevich@ThorntonTomasetti.com

Abstract

Vapor cloud explosions (VCEs) can cause significant damage to nearby buildings, facilities and infrastructure with potential loss of life and significant business interruption, so the accuracy of predicting blast loads on facility buildings is critical in estimating these losses. Closely spaced buildings and process equipment outside of the congested region of a VCE provide a complicated flow field for an expanding blast wave. Their presence can channel and shield the blast flow field, resulting in significant effects on the blast load magnitude and wave form shape. Currently, the most common way to estimate applied blast pressures resulting from VCE's is to use simplified methods that account for the total energy from the stoichiometric portion of the vapor cloud, fuel reactivity, and level of congestion and confinement, such as the TNO Multi-energy, equivalent TNT, CAM, and BST methods.

These simplified tools are based on unobstructed line-of-site conditions, which can overestimate and/or underestimate blast loads. This presentation illustrates the use of a fast-running Computational Fluid Dynamic (CFD) approach that can account for channeling and shielding effects without having to use a turbulent combustion model. This approach provides a convenient tool for designers and process safety planners to more accurately quantify the hazard from postulated VCE hazards that include site-specific channeling and shielding effects. The accuracy of the approach is demonstrated via comparisons of CFD simulations to experimentally measured waveforms. Computed pressure and impulse are also compared to the BST predictions for unobstructed and obstructed sites.

Key Words

Facility siting, VCE, CFD, blast pressure and impulse, petro-chemical facility safety

Approach

Our objective is to accurately and efficiently assess the VCE loads on structures in order to design the most effective and lowest cost retrofits possible. We seek to avoid the excess conservatism of some commonly used simplified approaches, while also avoiding areas where the simplified approaches underestimate the true loads. To compute loads on structures inside the congested and confined combustion region, a detailed CFD combustion analysis is required. This is an expensive and time consuming modeling effort which we do not address here.

The tools here apply outside of the vapor cloud combustion region where structural designers would typically estimate loads using TNO Multi-energy, equivalent TNT, CAM, or BST methods. The approach here is to develop an equivalent VCE source in a CFD code that produces the desired peak pressures, impulse and waveforms outside the combustion region where the structures of interest are located. This is in the class of CFD methods termed "Simplified Combustion Models in CFD" in (1). They note:

> *The advantage of this class of CFD VCE codes… is that the use of the flame speed table eliminates the effort of turbulent combustion modeling. The resolved mesh formulation adopted in the codes allows irregular geometries to be represented. The main application area for these codes is engineering-level analyses involving scenarios where blast wave shielding and focusing are relevant, such that simplified methods neglecting these effects would yield inaccurate results.*

The first step is to estimate the pressure and impulse versus range for an unobstructed site using one of the simplified methods. Here, we have chosen BST for illustration. The second step is to develop an equivalent VCE source in a CFD code. For this we use VCFD (2), a Thornton Tomasetti, Weidlinger Applied Science developed CFD code. For the VCE source we assume a hemispherical vapor cloud characterized by radius, energy per unit mass and constant flame speed relative to the ground. We use optimization software to tune the radius, energy and flame speed to best match the BST-derived peak pressures and impulse over the target ranges of interest. The optimizer automatically runs a sequence of 1D spherical VCFD calculations to tune the vapor cloud parameters. These run quickly. These assumptions have proven adequate to date, although 2D axisymmetric (or even 3D) vapor cloud geometries could be specified, and a constant flame speed need not be assumed.

With the optimized equivalent source as initial conditions, a fully 3D VCFD simulation may be performed to determine the blast loads on modeled structures while accounting for shielding, channeling, clearing and wrap-around effects automatically from nearby buildings and process equipment. It also produces a close approximation of the correct waveform, which can reduce the loads on the blast-facing structure sides and increase them on the shielded structure sides compared to an assumed shock waveform. The CFD approach naturally produces the negative phase as well, which is often neglected in simplified approaches. We emphasize again, that matching the BST pressure and impulse decay with range with a CFD code, will produce an appropriate waveform. The waveform will vary from a smooth slow rise at low pressure deflagrations, to a shock form at high flame speeds (see

Figure 3 and

Figure 4 below).

A fully coupled Finite Element/CFD analysis using NLFLEX (3) and VCFD (2) can also be computed if warranted. Structural damage and deformation is caused by pressure differences from the building exterior to the building interior. For flimsy structures such as trailers, pre-engineered metal buildings, tents, or buildings with openings such as open doors or breaking windows, the internal pressure will somewhat counteract the external pressure, thus reducing the net loads and causing less structural damage. On the other hand, negative phase pressures will have the reverse effect, as the internal pressure will push outward on the walls, causing potentially more structural damage.

The next section will demonstrate the method for determining initial input parameters for the calculation using fast-running 1D CFD methods, and validation versus test cases. The final section will show an example where the 1D input parameters have been used to perform analyses, demonstrating the advantages of this method over more simplified tools.

Validation

We have computed a selection of demonstration cases to verify that our method can adequately match the simplified-method pressure and impulse as a function of range, for low flame speed deflagrations through high speed detonations. We have also compared with experiments to validate that the waveforms are appropriate at both low and high pressures.

Figure 1 shows validation points superimposed on the BST curves. Here Mf is the flame speed relative to sound speed, OP/P_0 is scaled pressure, and R/R0 is scaled radius. The comparisons span the full range outside of the combustion region. A few typical comparisons are summarized here.

Figure 2 compares VCFD-calculated peak pressures and impulse vs. range to those obtained from the BST method for an example documented in (1). We note that there were errors in the calculated combustion energy in the published example which were corrected here.

Figure 3 compares VCFD-computed vs. experimental waveforms for a deflagration (4). Note the smooth waveforms and slow rise times, which are nothing like a shock. Likewise

Figure 4 compares waveforms for a detonation experiment (5) which does produce a shock-like waveform. For both cases, the physical behavior is properly and automatically reproduced by the CFD approach.

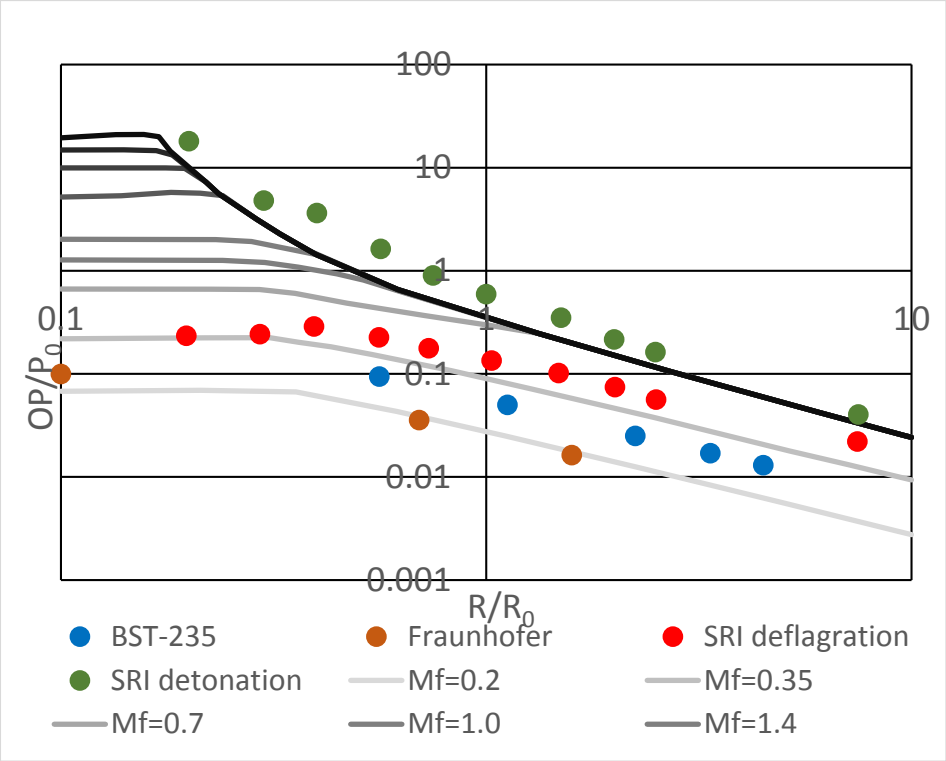

Figure 1. Validation cases relative to BST chart

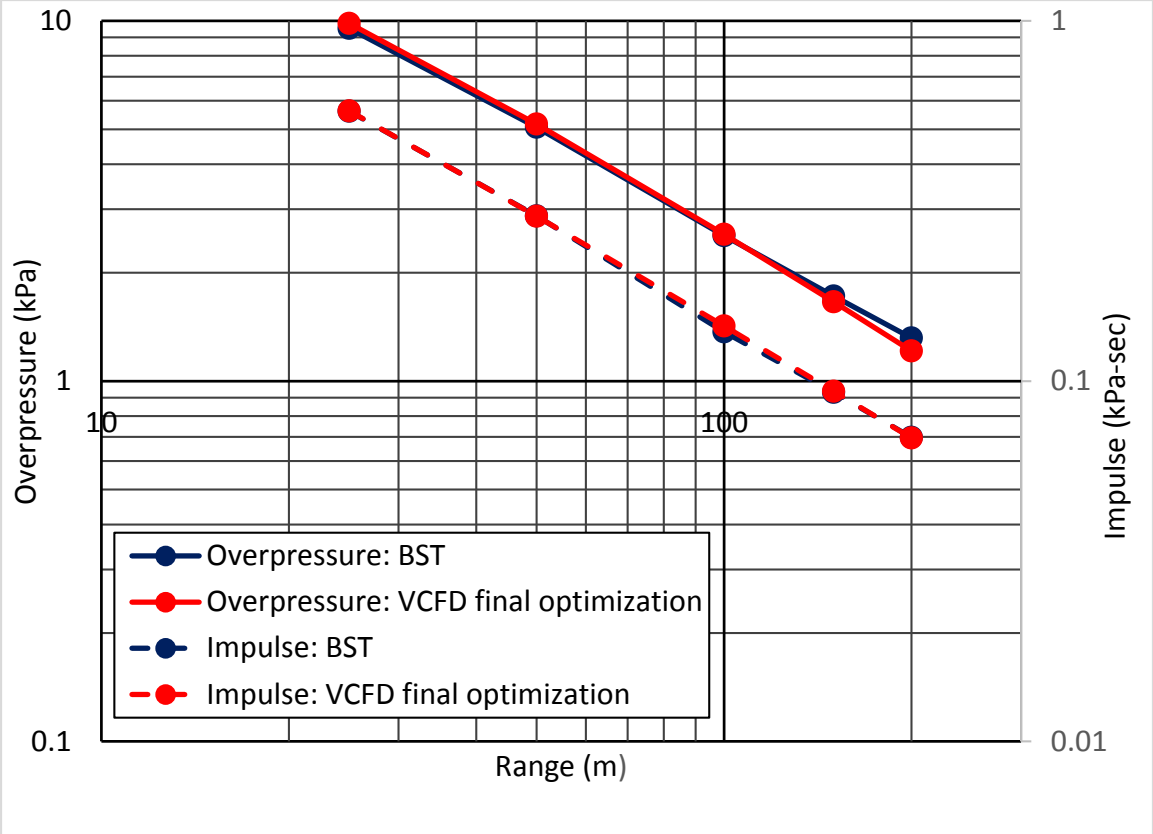

Figure 2 Simplified CFD Pressure and Impulse fit to BST

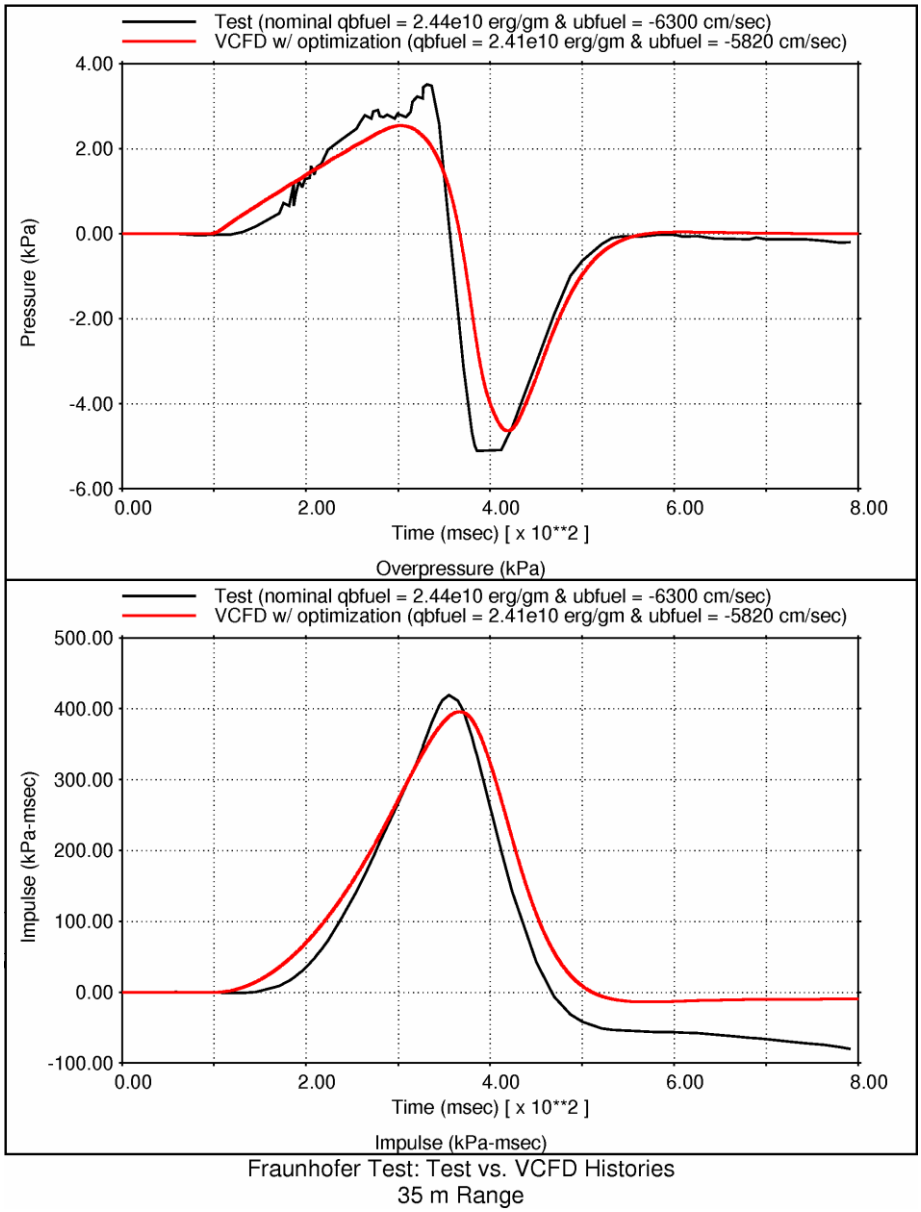

Figure 3. Deflagration waveforms compared to experiment – not shock like

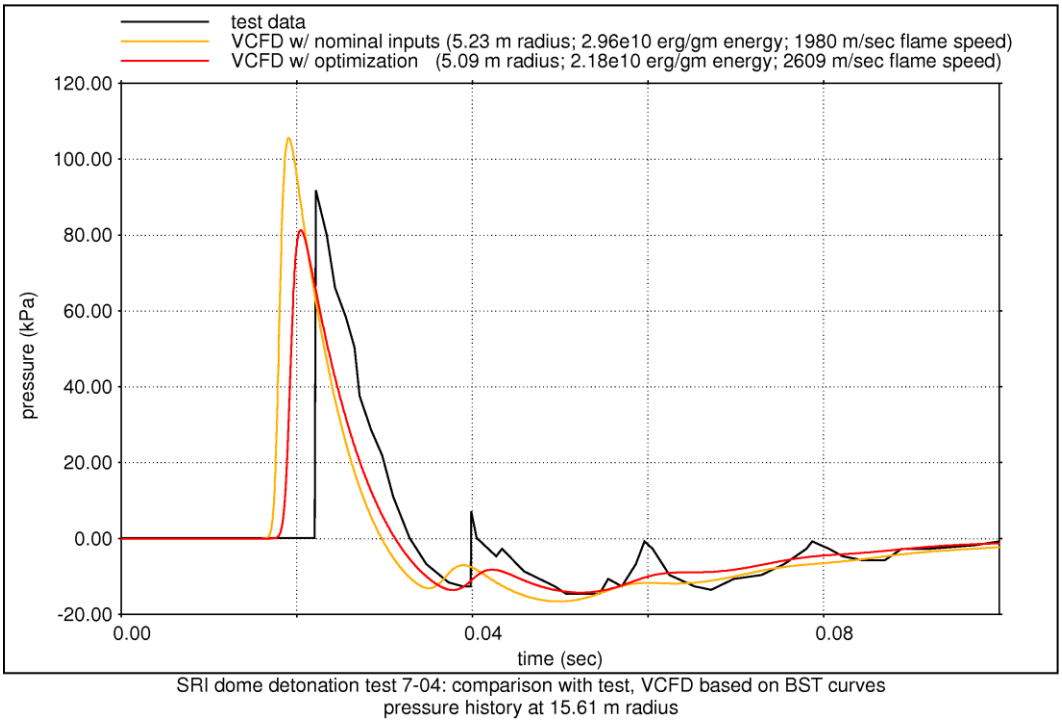

Figure 4. Detonation waveforms compared to experiment – shock like

Examples

In this section we compare the CFD approach to a well-accepted simplified approach provided by ASCE (6) for a hypothetical deflagration loading on a refinery central office building. The deflagration size and location are a purely fictitious representative example, but the building itself is based on an actual refinery office building as illustrated in Figure 5.

Figure 6 shows the peak pressure and impulse vs. range calculated by BST and the equivalent tuned approximation produced by the simplified CFD source. In this case the closest point of the building was assumed to be located about 40m from a VCE PES, and experiences a peak incident pressure of about 3 psi.

Figure 7 shows a snapshot of the blast wave sweeping over the structure at about 0.26 seconds after ignition. Figure 8 shows the peak overpressure distribution and Figure 9 shows the peak impulse distribution on the structure. As expected, the highest pressure regions are seen to occur on walls facing the blast.

Figure 10 shows a plan view of the building with a few gage points labelled for comparison. The structure is 4m high with a flat roof. The gage points are located at mid-wall height, or 2m above the ground.

Figure 11 compares CFD vs. simplified reflected pressures on the closest face of the building. The simplified peak pressure and impulse are larger, likely due to the assumed shock-like wave form and reduced clearing.

Figure 12 compares CFD vs. simplified pressures on the inside of the horseshoe. These are quite similar, except for neglecting the negative phase in the simplified approach.

Figure 13 compare simplified vs CFD pressure and impulse at an exterior corner. Here the simplified approach peak pressure is almost a factor of two too high.

Figure 14 compares pressure and impulse at the end of the horseshoe – again the simplified approach is high.

Figure 15 compares pressure and impulse on the back side of the building – here the simplified approach is substantially high which may be non-conservative when computing net loads on the building lateral resisting system.

Figure 5. Refinery Office Building at bottom center

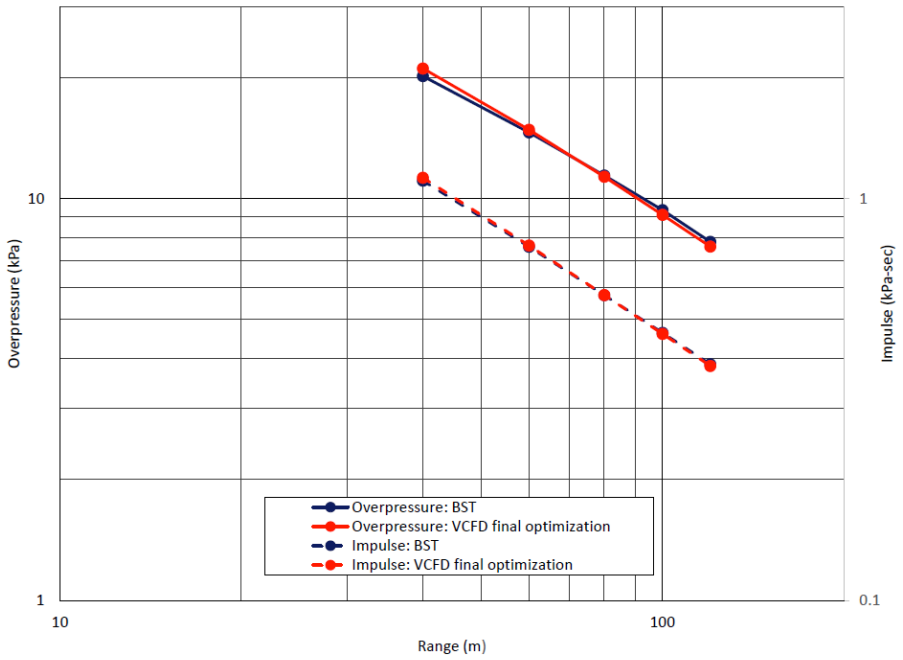

Figure 6. BST pressure and impulse for building example

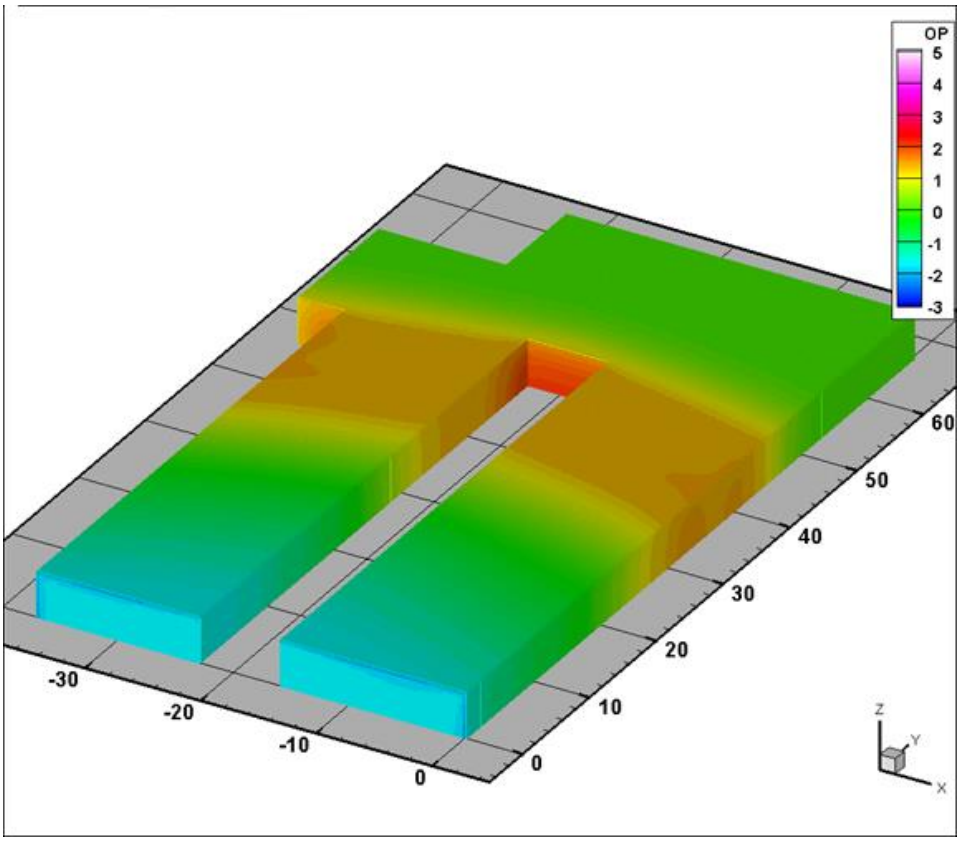

Figure 7. Snapshot of pressure wave sweeping over building

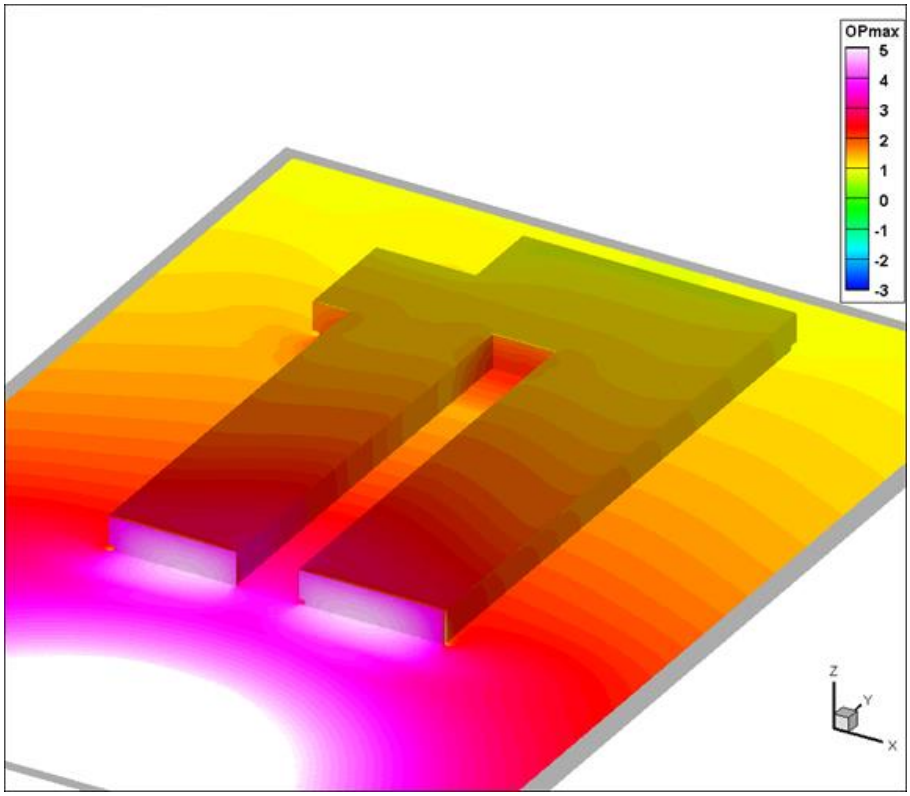

Figure 8. Peak reflected pressure distribution on building

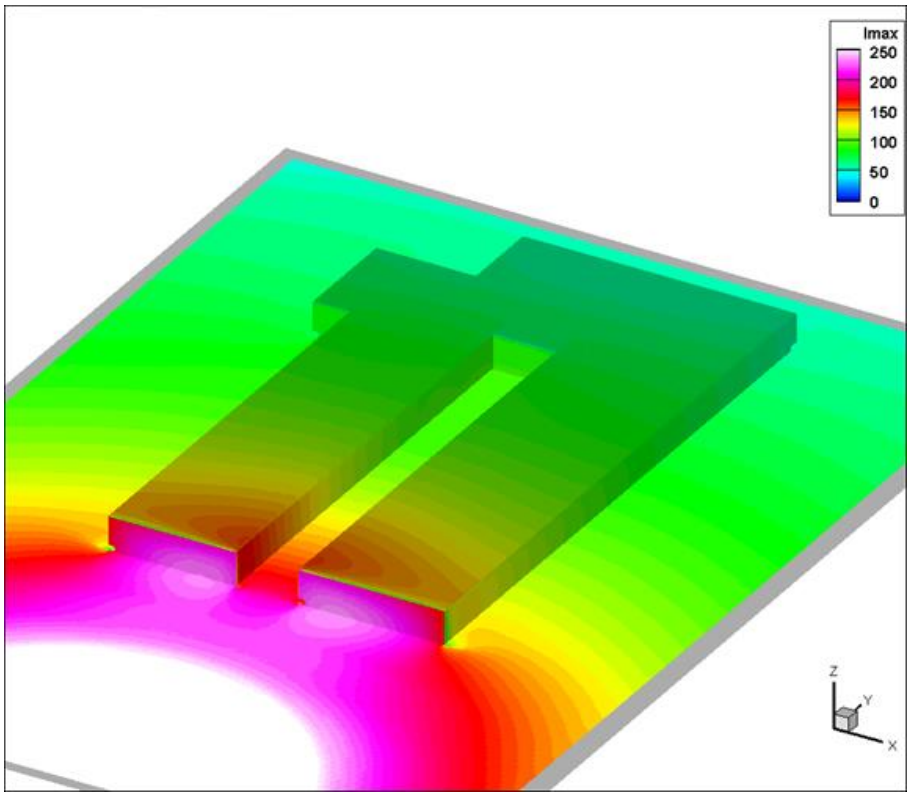

Figure 9. Peak computed impulse distribution on building

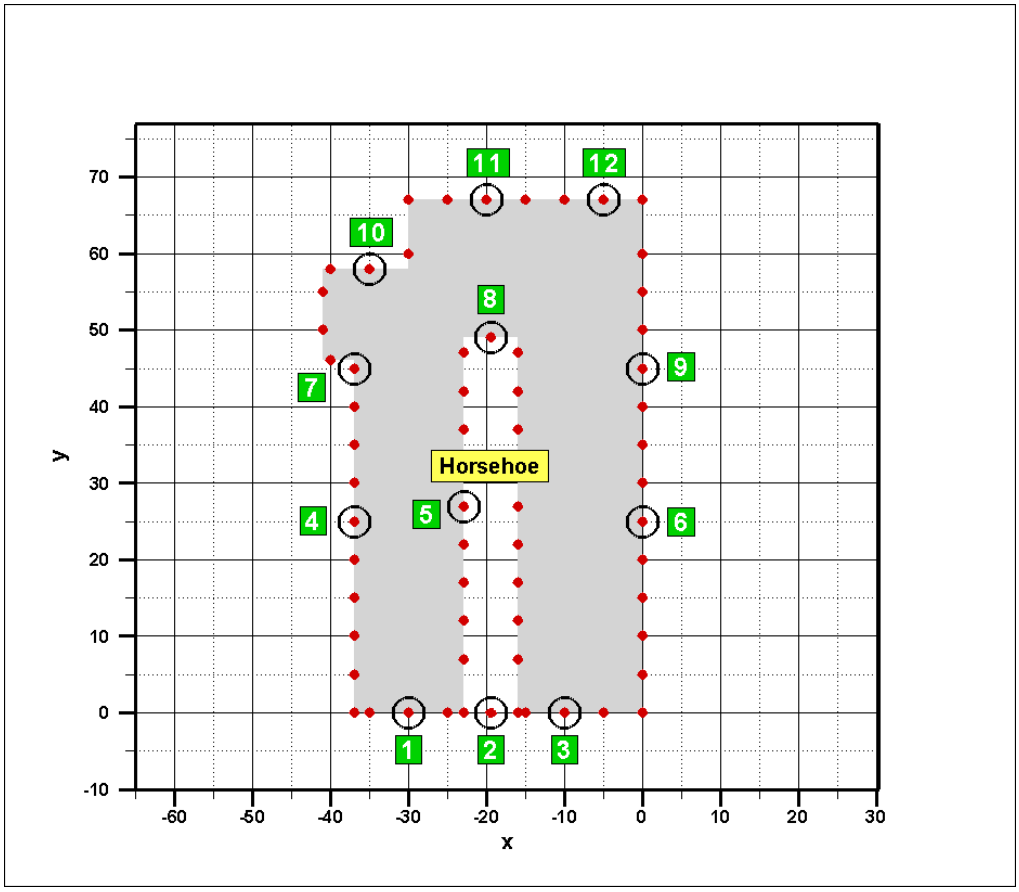

Figure 10. Gage points for comparison of CFD vs. simplified method

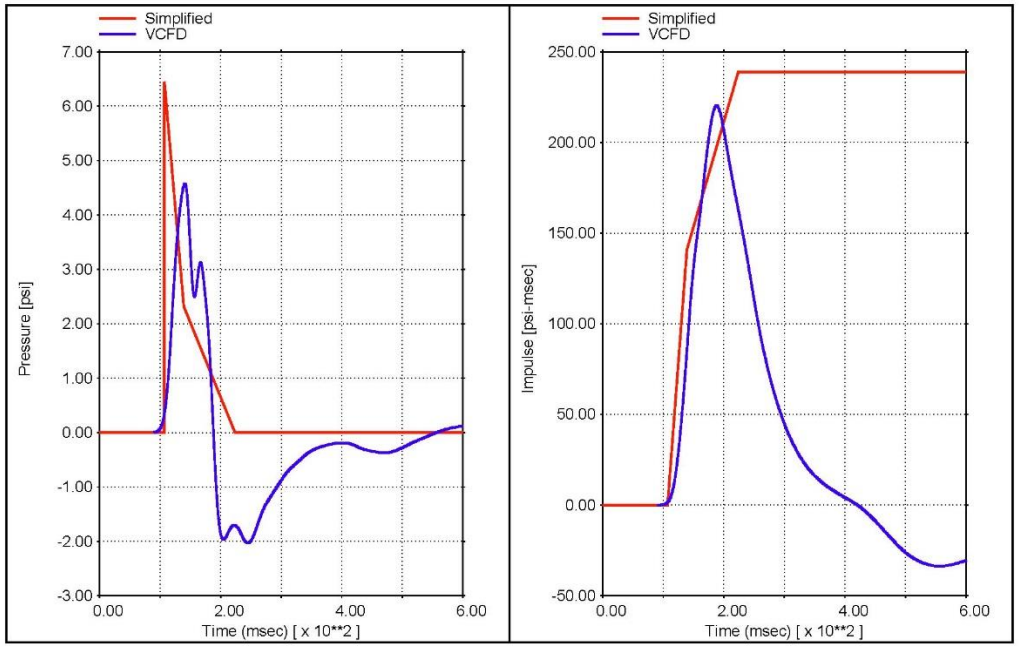

Figure 11. CFD vs. simplified reflected pressures at gage location 1

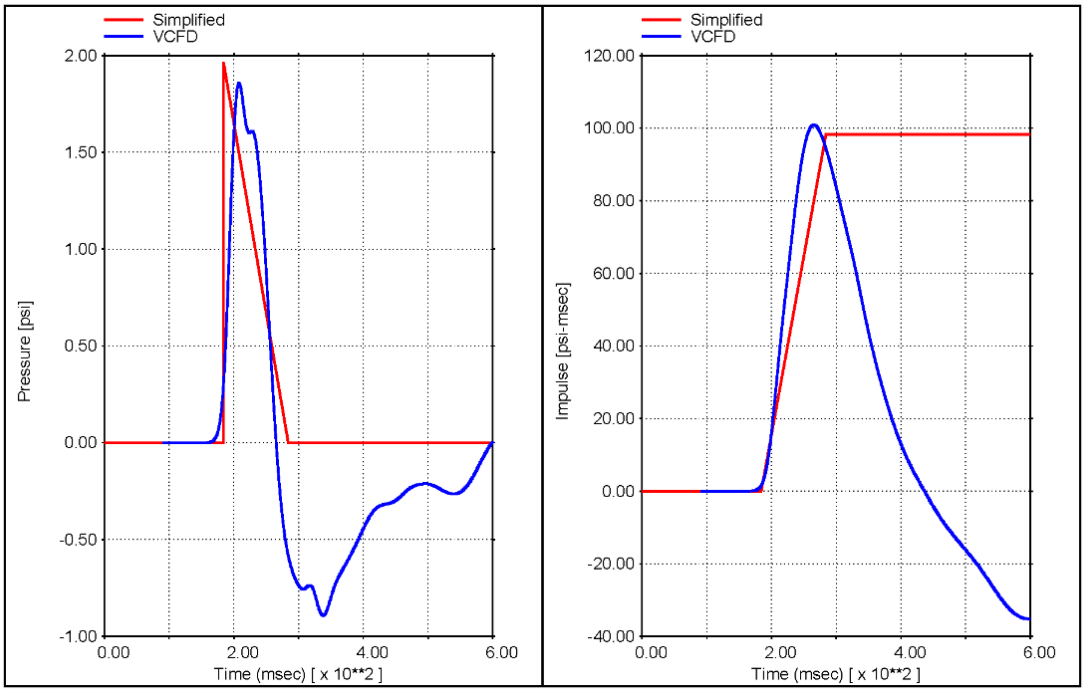

Figure 12. CFD vs. simplified pressures at gage location 5

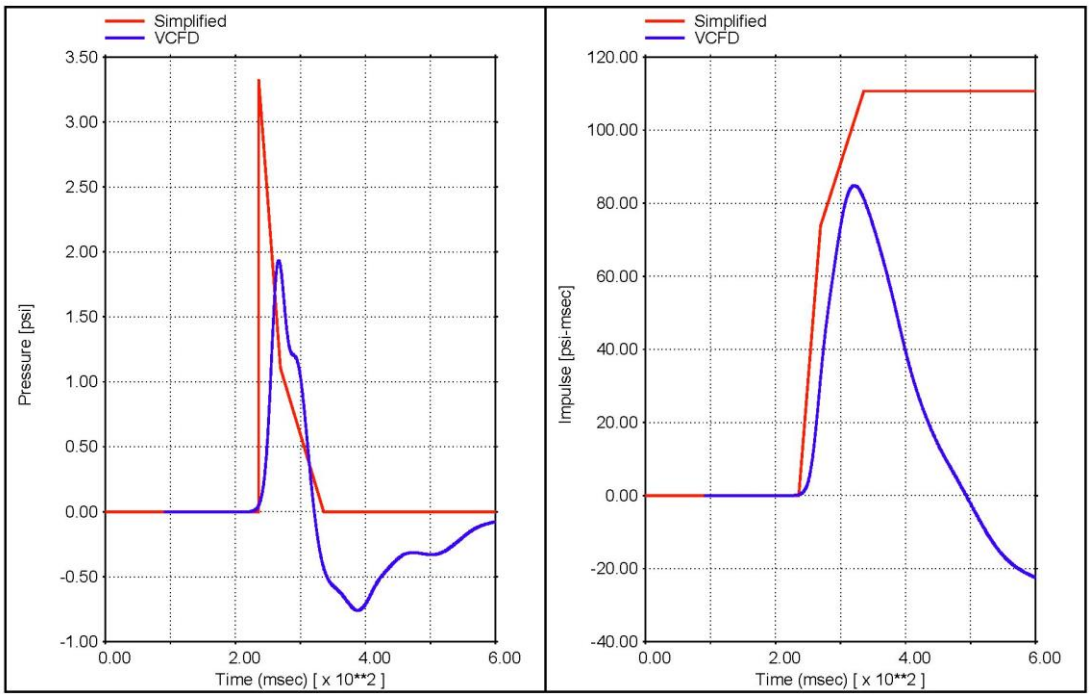

Figure 13 CFD vs. simplified reflected pressures at gage location 7

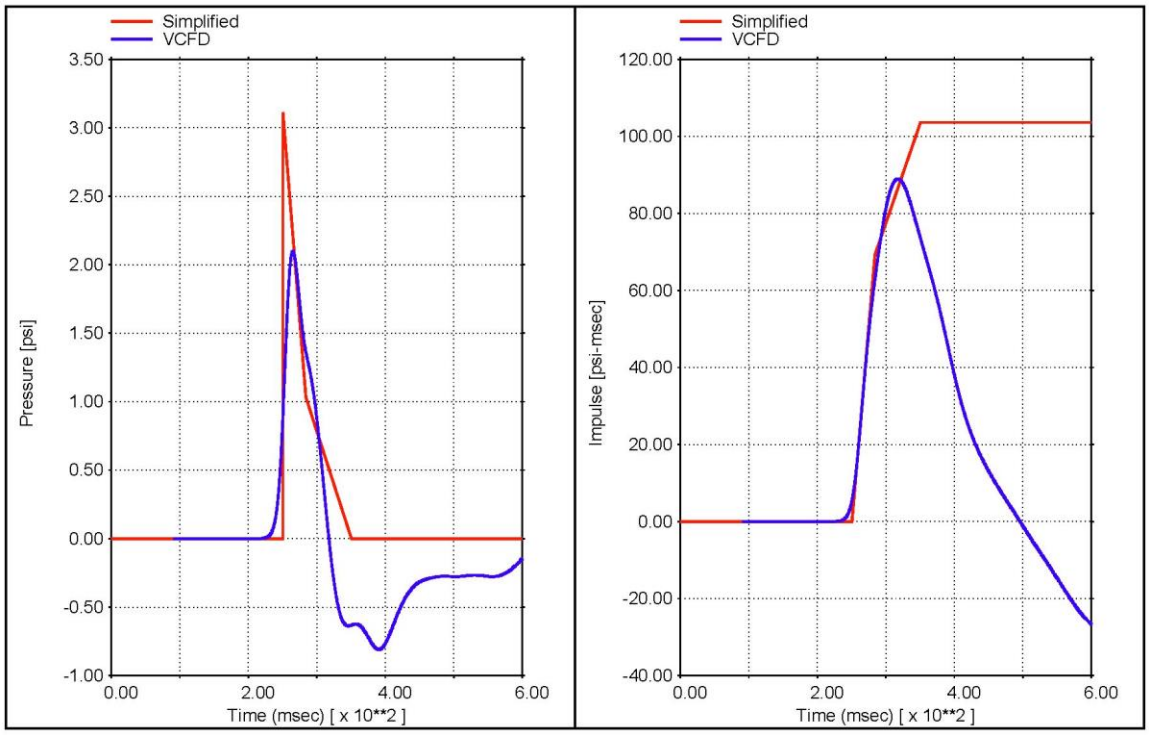

Figure 14. CFD vs. simplified reflected pressures at gage location 8

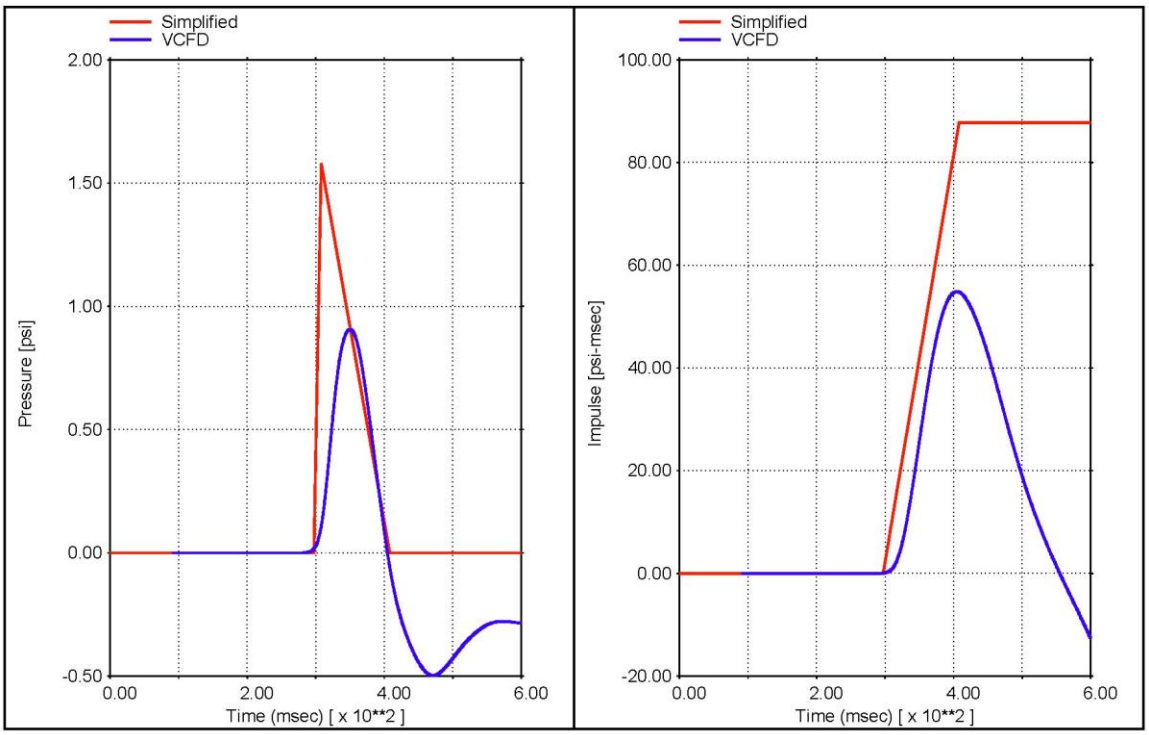

Figure 15. CFD vs. simplified pressures at gage location 11

Figure 16 shows the same building, loaded with the same blast but from a different direction in order to explore shielding effects. Figure 17 selects a few interesting gage locations for comparison.

Figure 18 compares reflected pressures on the wall facing the blast. The simplified peak pressure and impulse are a bit high. Figure 19 shows that the approximate pressure on the back side is high, but the impulses match well. Figure 20 shows the shielding effect of the front leg of the building on the back leg, which is neglected in the simplified approach.

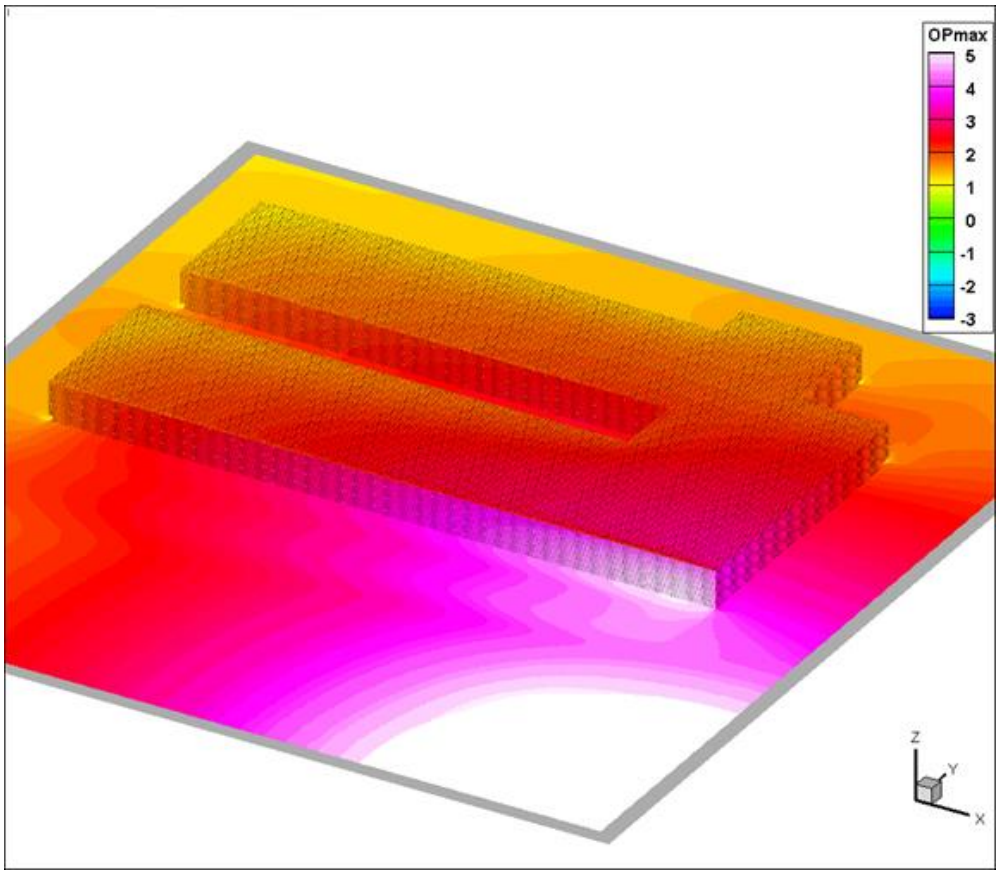

Figure 16. Refinery Building loaded from a different direction

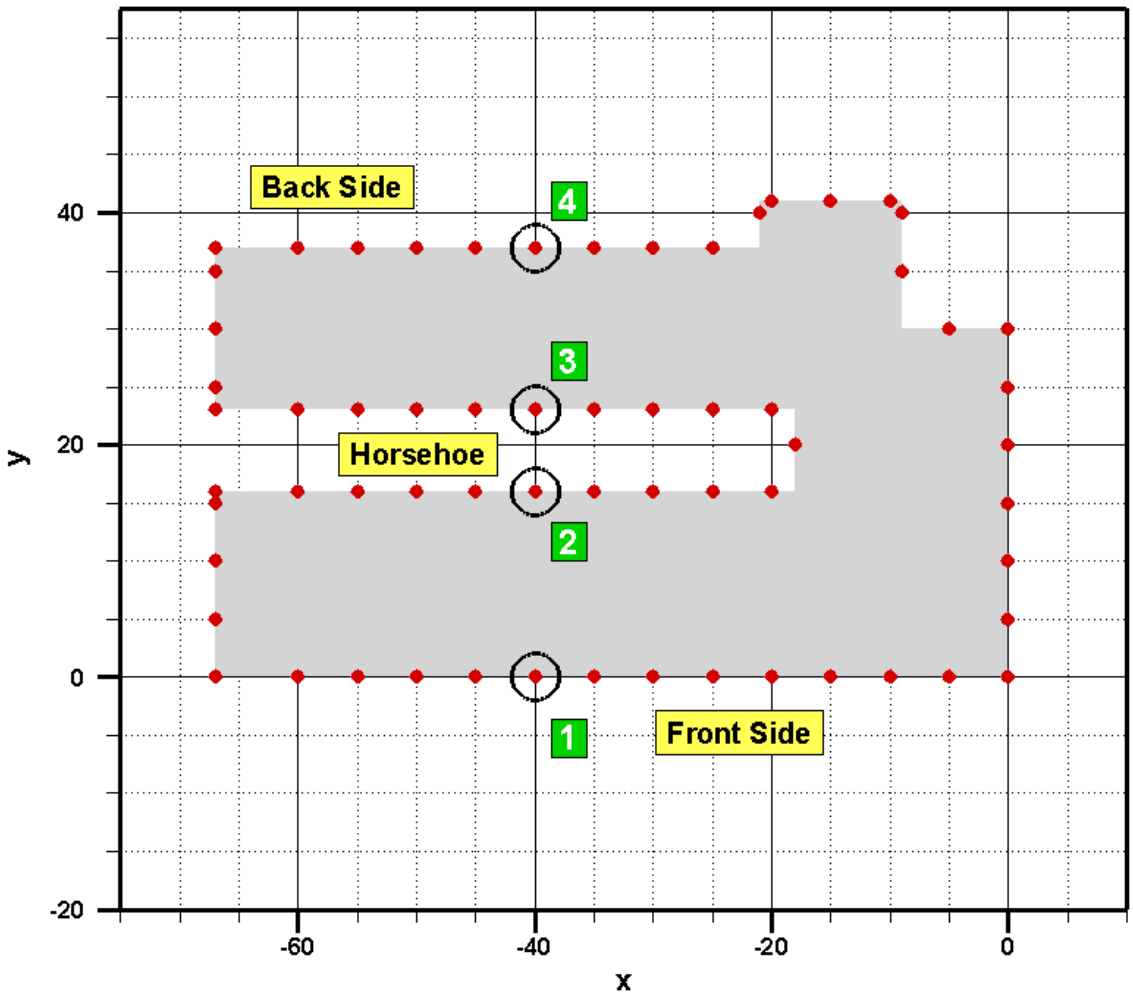

Figure 17. Gage location for shielding comparisons

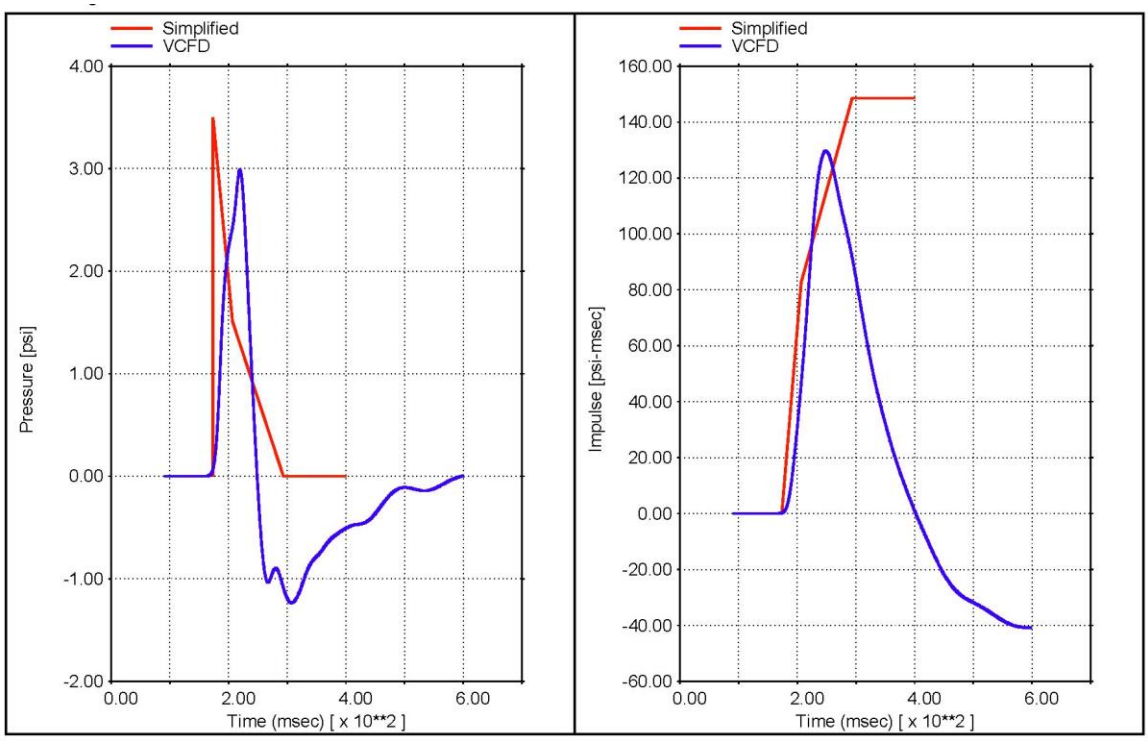

Figure 18. CFD vs. simplified reflected pressures at gage location 1

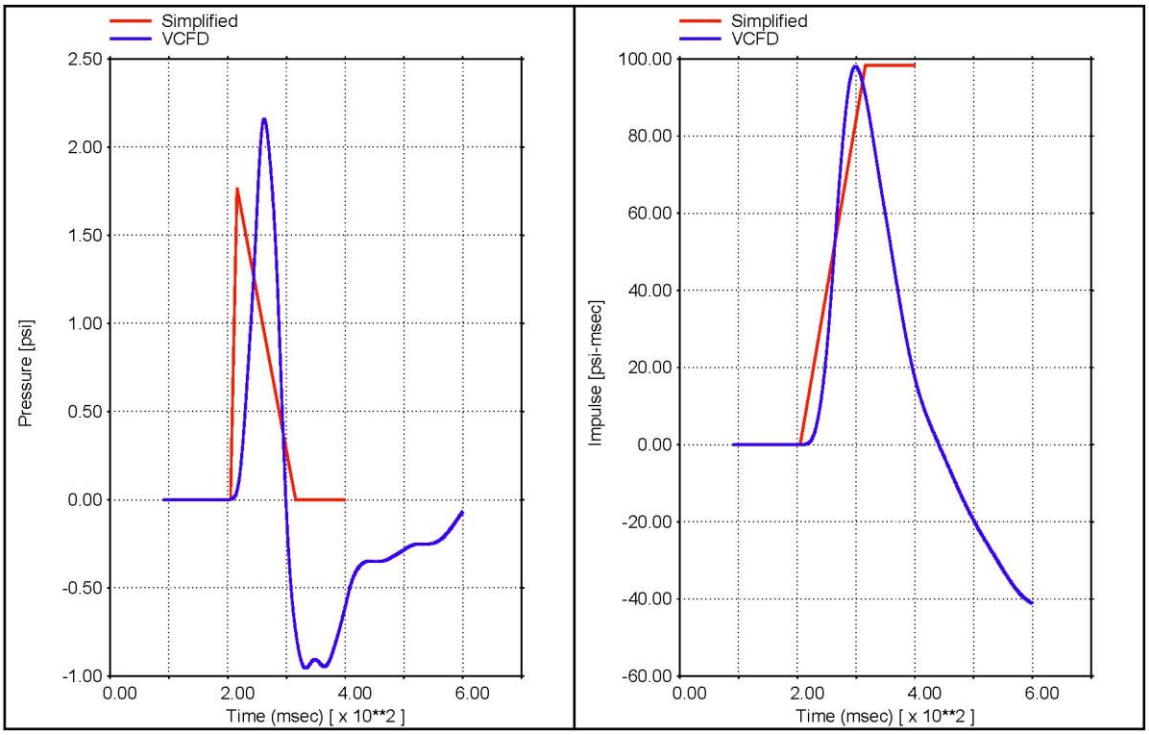

Figure 19. CFD vs. simplified pressures at gage location 2

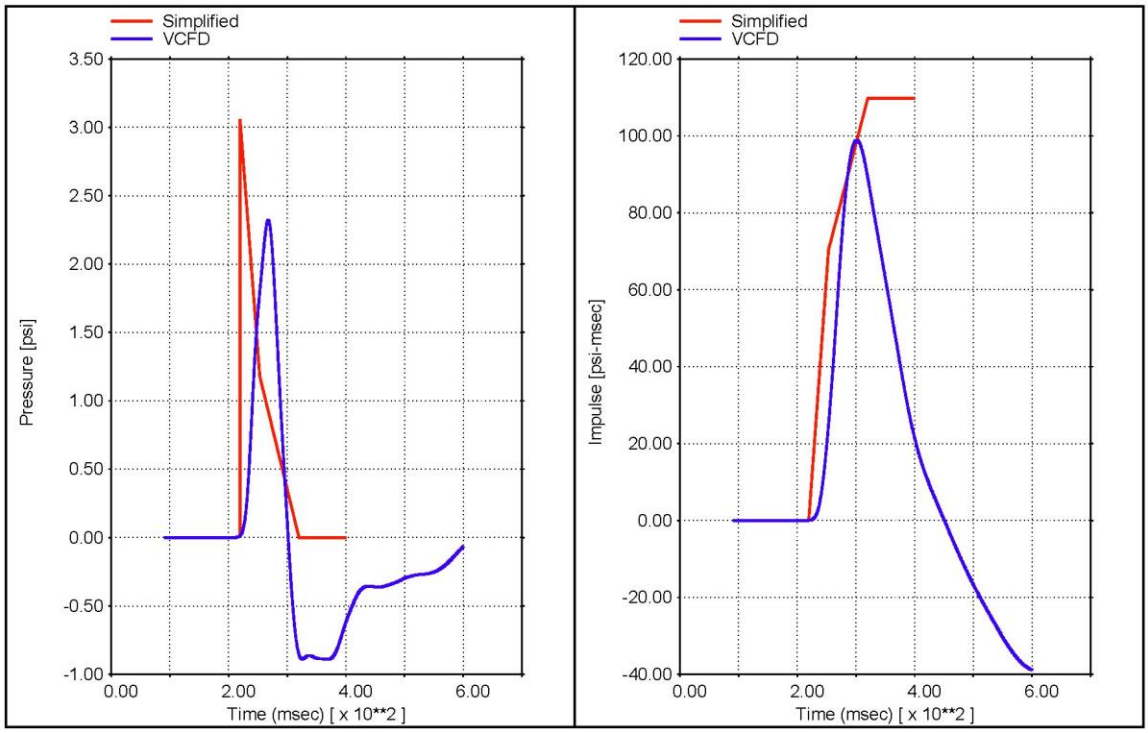

Figure 20. CFD vs. simplified reflected pressures at gage location 3

To demonstrate the effect of building height,

Figure 21 modifies the refinery building by increasing the front building wing height from 4m to 8m. Figure 22 through Figure 25 compare simplified vs. CFD waveforms for this case. The increased shielding effect from the taller building is evident by comparing Figure 24 to Figure 20. The simplified line of sight approach produces the same waveform, but the CFD approach captures the increased shielding. This same effect would be seen for adjacent upstream buildings if they were included in the 3D model.

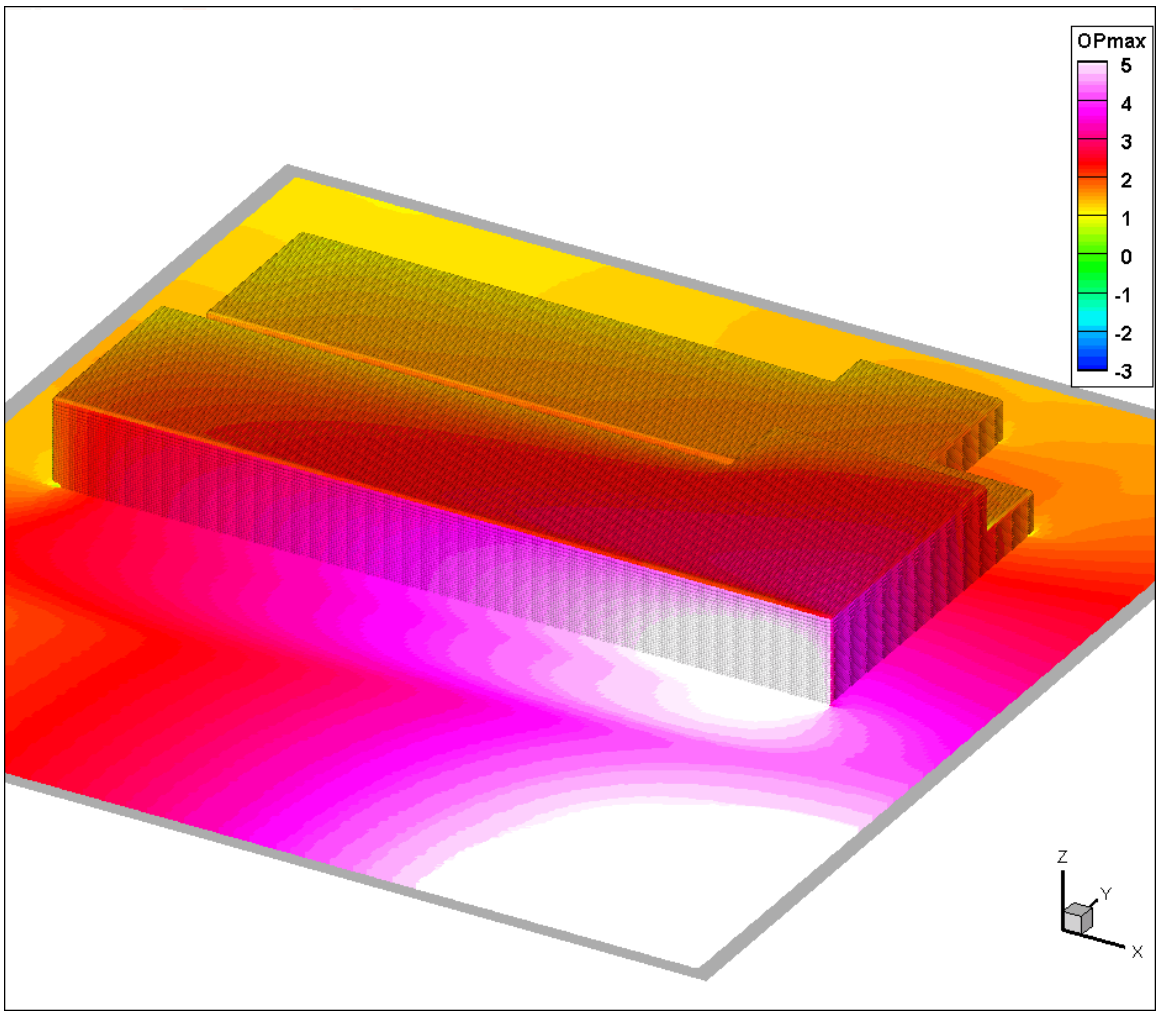

Figure 21. 8m Height Refinery Building loaded from a different direction

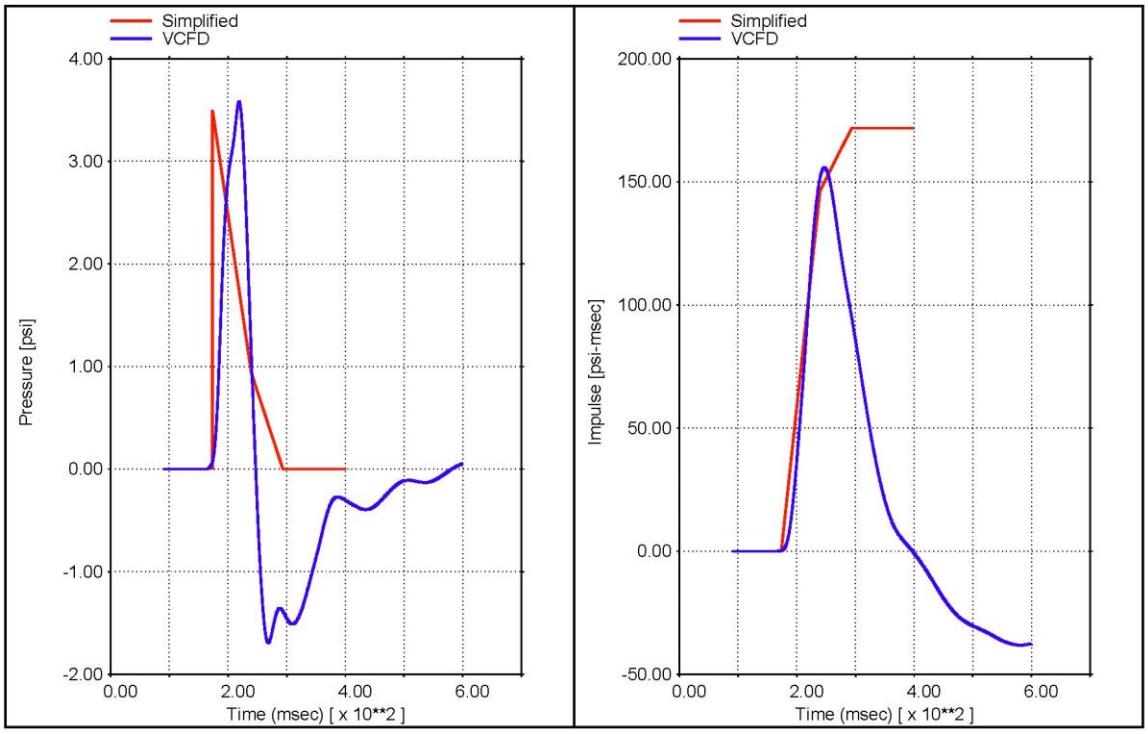

Figure 22. CFD vs. simplified reflected pressures at gage location 1 for taller building

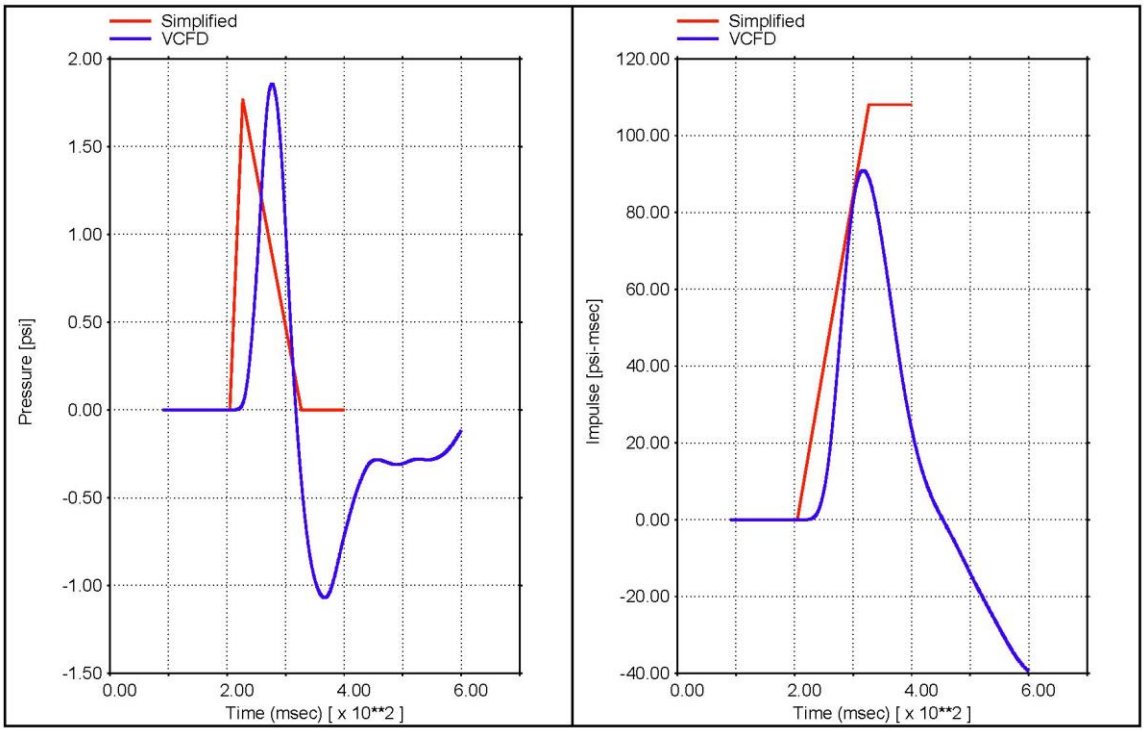

Figure 23. CFD vs. simplified pressures at gage location 2 for taller building

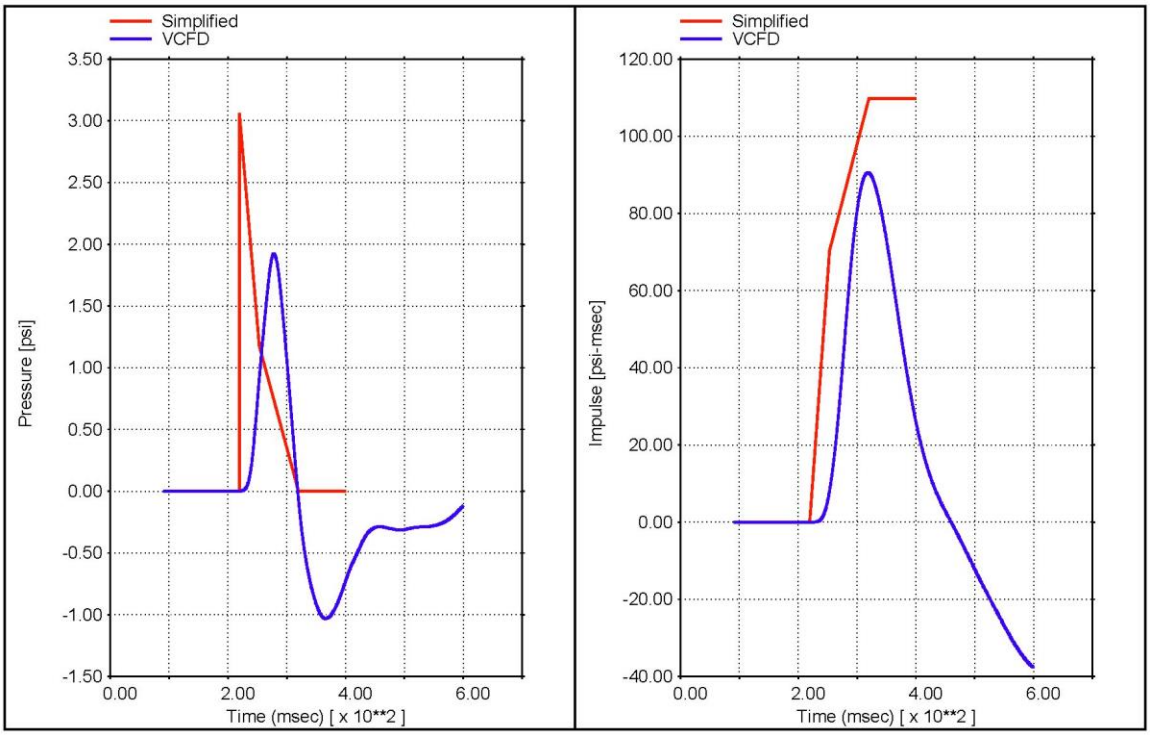

Figure 24. CFD vs. simplified reflected pressures at gage location 3 for taller building

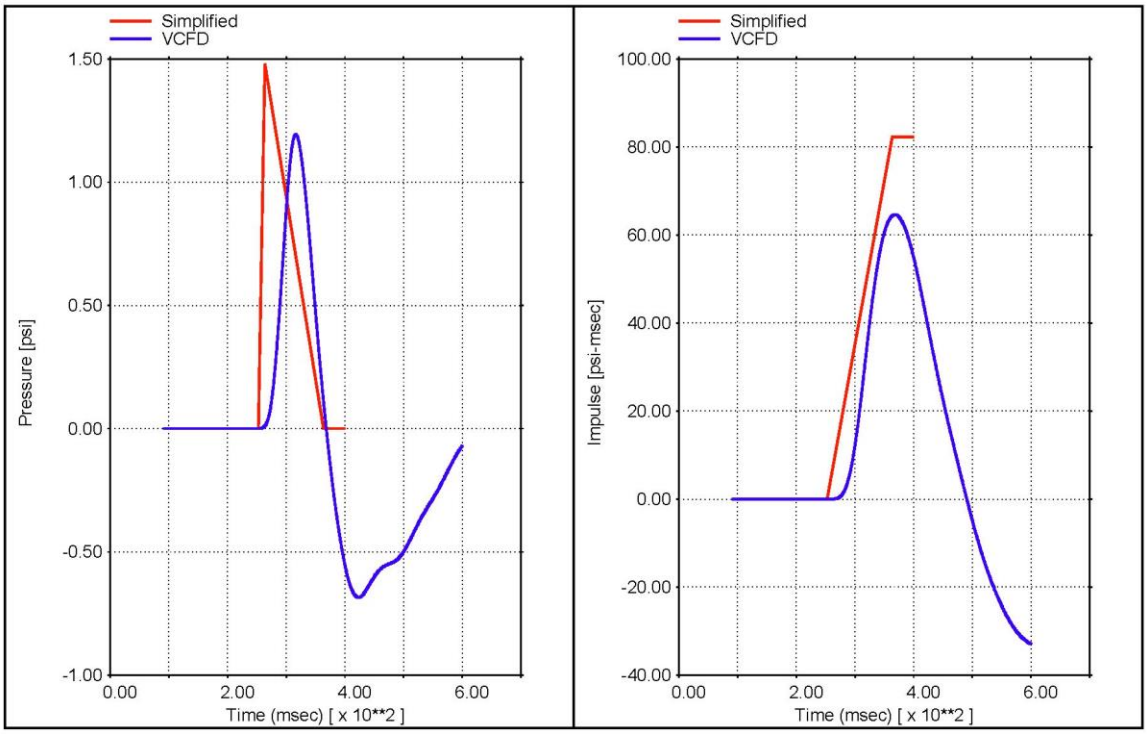

Figure 25. CFD vs. simplified pressures at gage location 4 for taller building

Summary

We have compared a simplified fast-running CFD approach to an accepted engineering level line of sight method for computing structural loads at petrochemical facilities based on the BST generated overpressures and their associated incident impulses. The CFD approach has advantages in that it removes excess conservatism, and automatically produces appropriate waveforms, reflection factors and negative phases.

Complex structures and neighboring buildings that produce shielding, multiple reflection and channeling effects (especially for shock like waveforms) are readily captured with the proposed CFD based approach.

Works Cited

1. Center of Chemical Process Safety. American Institure of Chemical Engineeers. *Guidlines for Vapor Cloud Explosion, Pressure Vessel Burst, BLEVE and Flash Fire Hazards.* Hoboken, NJ : John Wiley & Sons, 2010.
2. Hassig, P. *VCFD User Manual.* Cupertino, CA : Thornton Tomasetti, 2016.
3. Vaughan, D. *FLEX User's Guide, Report UG8298.* Mountain View, CA : Weidlinger Associates, May 1983 plus updates through 2016.
4. *Comparision of TNT-Equivalence Approach, TNO Multi-Energy Approach and a CFD Approach in Investigating Hemispheric Hydrogen-Air Vapor Cloud Explosions.* Beccantini, A., A. Malczynski, E. Studer. Edinburgh, UK : s.n., 2007. Proceedings of the 5th International Seminar on Fire and Explosion Hazards. pp. 23-27.
5. *Large-Scale hydrogen deflagrations and detonations.* Groethe, M., E. Merilo, J. Colton, S. Chiba, Y. Sato, H. Iwabuchi. 2007, International Jnl. of Hydrogen Energy, pp. 2125-2133.
6. Bounds, W.L. *Design of Blast-Resistant Buildings in Petrochemical Facilities.* s.l. : ASCE, 2010.
7. *Deflagration Safety Study Of Mixtures Of Hydrogen And Natural Gas In A Semi-open Space.* Merilo, E., M. Groethe. San Sebastian, Spain : s.n., 2007. HySafe 2007. Proceedings of the 2nd International Conference on Hydrogen Safety.